

Design of Model Predictive Controller for Trajectory Tracking of a Ground Station Antenna

M. Sarlak¹, M. Tavakoli², M. Sepehri^{3*}

Received :2015/10/20 Accepted: 2015/12/5

ABBREVIATION AND NOMENCLATURE

<i>AZ</i>	<i>Azimuth</i>
<i>EL</i>	<i>Elevation</i>
<i>PMSM</i>	<i>Permanent Magnet Synchronous Motors</i>
<i>LEO</i>	<i>Low Earth Orbit</i>
<i>GEO</i>	<i>Geostationary Earth Orbit</i>
<i>STS</i>	<i>Satellite Tracking Station</i>
<i>PI</i>	<i>Proportional Integral</i>
<i>DSP</i>	<i>Digital Signal Processor</i>
<i>MPC</i>	<i>Model Predictive Control</i>
<i>FL</i>	<i>Feedback Linearization</i>
<i>DH</i>	<i>Denevite Hertenberge</i>
<i>d-q</i>	<i>direct-quadrature</i>
<i>P</i>	<i>Number of pole pairs;</i>
<i>R</i>	<i>Stator resistance</i>
<i>L</i>	<i>Stator inductance</i>
θ	<i>Rotor position</i>
ω	<i>Angular velocity</i>
B_v	<i>Viscous friction coefficient</i>
<i>J</i>	<i>Moment of inertia</i>
T_L	<i>Load torque</i>
i_q, i_d	<i>Stator current in d-q frame</i>
v_q, v_d	<i>Stator voltage in d-q frame</i>
Φ_{mg}	<i>Flux of the permanent magnet</i>
ρ	<i>Air density</i>
A_f	<i>Affective area of the reflector in m²</i>
C_D	<i>Aerodynamic coefficient</i>
<i>V</i>	<i>Reflector speed (m/s)</i>
V_{wind}	<i>Wind speed (m/s)</i>
θ_{EL}	<i>Elevation angle</i>
θ_{AZ}	<i>Azimuth angle</i>
<i>ISE</i>	<i>Integral Square Error</i>
T_s	<i>Sampling time</i>

Abstract

This paper develops new results on the use of model predictive control to regulate the attitude of a ground station antenna. Two degree of freedom AZ-EL pedestal is considered as ground station antenna. Permanent Magnet Synchronous Motors are taken into consideration as the best choice for satisfaction of control objectives as actuators. The design is based on a two cascade controller consist of MPC and a simple feedback linearization, respectively. The proposed approach provides more smooth tracking and lower energy consumption with respect to analogous works. The model predictive controller employs integral action, resulting in zero steady-state error and load torque disturbance rejection. Realistic disturbances caused by wind and load is considered and applied to an industry-sized pedestal. The reference data of azimuth and elevation angles are chosen from a real tracking mission. The comparison of simulation results by typical PI controller, verify the effectiveness of the proposed method.

Keywords: tracking, azimuth-elevation pedestal, MPC, PMSM drive.

1. INTRODUCTION

LEO satellites offer several advantages over their GEO cousins. Compared to a GEO, a LEO satellite has lower launch costs, reduced power requirements and a significantly reduced roundtrip transmission delay. While a constellation of GEOs can only see earth stations with latitudes less than 81°, the use of polar orbits allows a LEO constellation to communicate with all points on the globe [1].

A STS must be able to track a satellite at any position in the sky above a few degrees elevation. The best quality of data reception is obtained when the telemetry signal is stronger, i.e., where the satellite is closest to the ground station. In addition, it is most important that the station can be capable of continuing a good tracking through and near the local zenith to assure quality reception of the telemetry data [2], [3]. The pedestals are one of the important parts of each STS. The most common and well-known type of pedestals are the elevation over azimuth pedestals. The keyhole problem in an AZ-EL pedestal occurs when the payload is tracking a satellite near its zenith position. The AZ-EL pedestals are unable to track continuously in cross of high elevation,

1. Bagherolloom Organization. iran.robotics@yahoo.com
 2. Bagherolloom Organization. hedayat.robotic@yahoo.com
 3. Master of Science Student, School of Electrical and Computer Engineering, University of Tehran, Tehran, Iran.
m.sepehrimovafegh@yahoo.com

because in this point, the difference of azimuth angle after zenith is 180° in comparison with prior azimuth angle before zenith, So it is necessary for azimuth's motor to turn the antenna during a short time [4]. Electric motors are in charge of putting the pedestal's reflector in the desired point. Therefore, it is important to choose the best kind of electric motor and design its drive carefully.

Permanent Magnet Synchronous Motors, which possess the characteristics of high power density, torque-to-inertia ratio, and efficiency, have been widely used in many industrial applications. Linear control schemes, are widely applied for the PMSM system due to their relative simple implementation [4-7]. In fact, nonlinear behavior of PMSM system in the presence of disturbances, as well as parameter variations, make it difficult for linear controllers to maintain system performance and even stability.

Some research have reported the weakness of PI control algorithm to satisfying dynamic behavior in the entire operating range [12]. Thus, advanced control algorithms, are a natural solution.

The required calculation time due to the nature of nonlinear algorithms was one of the major impediment existed to apply advanced control methods to the power electronic systems with high sampling rate. Although, this issue is partly obviated by the advent of powerful processors like DSPs.

There are many researches to develop nonlinear control methods for the PMSM, and various algorithms have been proposed, e.g., adaptive control [9,11,17], robust control [10,12], sliding-mode control [13] as well as intelligent control [14,18,22].

However, most of the control strategies proposed in relevant literature do not pay attention to experimental considerations, such as *dynamics* and *saturation limits* of the actuators, which might cause input signal to exceed an admissible value and result in either loss of performance or even crushing of system.

An interesting alternative to satisfy such a requirement is utilizing model predictive control, which provides some advantage over the other method such as: (i) The multivariable case can easily be deal with, (ii) The resulting controller is easy-to-implement, (iii) Its extension to the treatment of constraints is conceptually simple, and these can be systematically included during the design process [21]. Briefly, MPC strategy is to calculate a set of future control signals by

optimizing a determined criterion to keep the process as close as possible to the reference trajectory. An explicit solution can be obtained if the criterion is quadratic, the model is linear, and there are no constraints; otherwise an iterative optimization method has to be used. In each instant, only the first element of computed control sequence $u(t)$ is sent to the process and at the next time sample the same steps repeated with the new measurement of system [21].

In this paper an AZ-EL pedestal is considered as controlled system (Fig. 1). Two PMSMs are employed as actuators for each AZ and EL angles. System stability in the presence of wind



Fig. 1. AZ-EL pedestal

-gust and excessive loads as disturbance are ensured by steering all signals in an admissible region. In order to exploiting of the all capacities of MP controller with imposing no restrictive assumption to the system, a feedback linearization is employed. Concisely, the main contributions of this paper over the analogous works can be itemized as follow:

- Dealing with original nonlinear model without any locally linearization to prevent interfering model mismatch destructive effects
- Provision a versatile MP controller for all operating points with the high performance and lower energy consumption, during tracking mission
- Analysis of the forces produced by load and wind and considering during simulation

Eventually, this paper is structured as follow: Section 2 is dedicated to modeling of system. In section 3, the proposed control strategy is discussed. Section 4 devoted to the analysis of the

forces produced by load and wind. Pedestal system operation is described in section 5. A comprehensive simulation is performed in section 6. Finally, conclusion is drawn in section 7.

2. System Modelling

Because of AZ-EL pedestal structure, system coordination does not need to be transformed into a secondary coordination using DH equations (Fig. 2). Therefore, it is enough to only extract the model of motors and the gear boxes besides to the reflector and atmosphere conditions such as wind speed.

Among all pedestal's component, electrical motors are the main section to be modeled and controlled. PMSMs are appropriate choice according to their high efficiency, construction and maintenance costs with respect to other types. Taking the rotor coordinates (d-q axes) of the motor as reference coordinates, the model of a surface-mounted PMSM can be described as [5]:

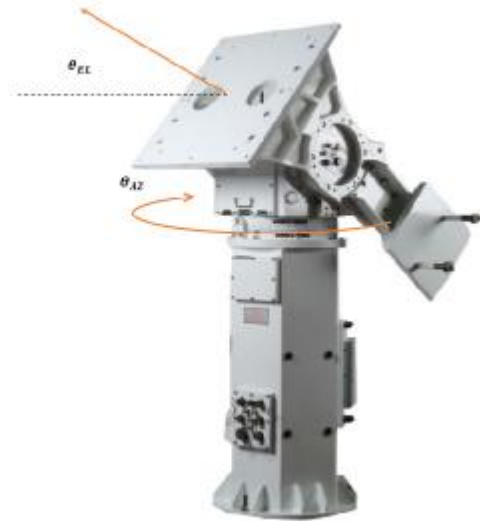


Fig. 2. AZ-EL angles

$$\begin{aligned} \frac{d\theta}{dt} &= \omega \\ \frac{d\omega}{dt} &= \frac{P}{J} \left(T_e - \frac{B_v}{P} \omega - T_L \right) \\ \frac{di_q}{dt} &= \frac{1}{L_q} (v_q - Ri_q - \omega L_d i_d - \omega \phi_{mg}) \\ \frac{di_d}{dt} &= \frac{1}{L_d} (v_d - Ri_d + \omega L_q i_q) \end{aligned} \quad (1)$$

Where $T_e = \frac{3}{2} p [\phi_{mg} i_q + (L_d - L_q) i_d i_q]$

3. Controller design

With regards to the proportional integral controllers' performance in position control of PMSMs, significant efforts have been done in order to use modern controllers for having better tracking accuracy.

In this section, a model predictive control technique is proposed for the closed-loop position control system for permanent magnet synchronous motors as the most important parts of the AZ-EL pedestal system model. The control sequence for the predefined path tracking by starting from an initial condition is illustrated in Fig. 3

a) System Dynamic

Equation 1 can be expressed in terms of the following equations

$$\begin{aligned} \dot{x}_m &= Ax_m + Bu \\ &+ d(k) \end{aligned} \quad (2)$$

$$y = Cx_m;$$

$$\text{where } x_m = \begin{bmatrix} \theta \\ \omega \end{bmatrix} \quad A_m = \begin{bmatrix} 0 & 1 \\ 0 & -\frac{B_v}{J} \end{bmatrix} \quad B_m = \begin{bmatrix} 0 \\ 1 \end{bmatrix}$$

$$C_m = [1 \ 0] \quad u = \frac{3}{2J} P^2 [\phi_{mg} i_q + (L_d - L_q) i_d i_q]$$

$$d(k) = \frac{P}{J} T_L(k)$$

It must be noted that variable u in the Eq. 2 is a virtual controlling input. By assigning the $i_d^* = 0$, the i_q^* as a reference of i_q variable will be obtained. The current references must be satisfied through the input voltages v_q and v_d in the following equation:

$$\frac{di_q}{dt} = \frac{1}{L_q} (v_q - Ri_q - \omega L_d i_d - \omega \phi_{mg}) \quad (3)$$

$$\frac{di_d}{dt} = \frac{1}{L_d} (v_d - Ri_d + \omega L_q i_q)$$

b) MP Controller Design

The MPC design used in this paper is from [20], where is specialized to the case of position regulation for a PMSM.

In common with the PI control scheme, an integrator is embedded in the MPC design, which is also used for the following purposes: (i) elimination of motor parameters uncertainty, and

(ii) removal of the load disturbance torque which is assumed to be an unknown constant. This is the first step and once complete the MPC design is undertaken using the incremental model where the defining vectors are the differences among the state, input and output vectors, respectively, for any two successive sample instants. Therefore, when the operating conditions change it is only necessary to update the set-point signals to reflect this change and the other steady-state values for the state variables are not required. However, the parameters in the system matrices (2) depend on the operating conditions and if these undergo a drastic change, parameter updating may be required, resulting in a gain scheduled predictive controller [19].

Let $\Delta x_m(k) = x_m(k) - x_m(k - 1)$ and $\Delta u(k) = u(k) - u(k - 1)$ denote the incremental state and input vectors, respectively, computed from the corresponding vectors in (2). Then, the state dynamics in the incremental model are described by:

$$\begin{aligned} \Delta x_m(k + 1) &= A_m \Delta x_m(k) + B_m \Delta u(k) \\ y(k + 1) - y(k) &= C_m A_m \Delta x_m(k) + C_m B_m \Delta u \end{aligned}$$

and the augmented state-space model for design takes the following form:

$$\begin{aligned} x(k + 1) &= Ax(k) \\ &+ B\Delta u(k) \\ y(k) &= Cx(k) \end{aligned} \tag{4}$$

$$\begin{aligned} \text{Where } x(k) &= \begin{bmatrix} \Delta x_m(k) \\ y(k) \end{bmatrix} & A &= \begin{bmatrix} A_m & \mathbf{0} \\ C_m A_m & \mathbf{1} \end{bmatrix} \\ B &= \begin{bmatrix} B_m \\ C_m B_m \end{bmatrix} & C &= [\mathbf{0} \ \mathbf{0} \ \mathbf{1}] \end{aligned}$$

One advantage of this model is removal of the nearly constant and unknown load T_L from the design.

By means of Eq. 4 the future outputs of the model take the following form

$$\begin{aligned} Y &= Fx(k) \\ &+ G\Delta U \end{aligned} \tag{5}$$

Where $Y = [y(k + 1) \dots y(k + N_p)]^T$

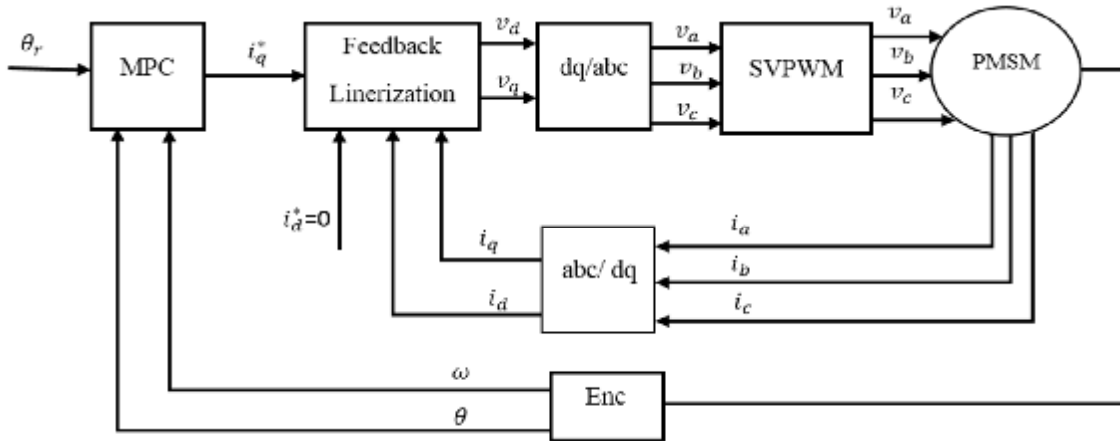


Fig. 3. Overall MPC-based control strategy

$$\Delta U = [\Delta u(k) \ \Delta u(k + 1) \ \dots \ \Delta u(k + N_u - 1)]^T$$

$$\begin{aligned} F &= [(CA)^T \ (CA^2)^T \ \dots \ (CA^{N_p})^T]^T \\ &= \begin{bmatrix} G & & & \\ C & \mathbf{0} & \dots & \mathbf{0} \\ CAB & CB & \dots & \mathbf{0} \\ \vdots & \vdots & \ddots & \mathbf{0} \\ CA^{N_p-1}B & CA^{N_p-2}B & \dots & CA^{N_p-N_u}B \end{bmatrix} \end{aligned}$$

Then cost function used for the MPC design has the structure

$$\begin{aligned} J &= (Y_r - Y)^T Q (Y_r - Y) \\ &+ \Delta U^T R \Delta U \end{aligned} \tag{6}$$

Where in this case $Y_r = [\mathbf{1} \ \mathbf{1} \ \dots \ \mathbf{1}]_{1 \times N_p}^T y_r(k)$

Under the receding horizon principle, the control vectors for the next N_u sampling instants are obtained by minimizing the cost function (6) but

only the first of these is applied to the plant. In the absence of constraints the global optimal solution is given by

$$\begin{aligned} \frac{\partial J}{\partial \Delta U} = \mathbf{0} &\rightarrow \Delta U^* \\ &= (G^T Q G + R)^{-1} G^T Q (Y_r \\ &\quad - Fx(k)) \end{aligned} \quad (7)$$

And the increment of the input at the instance t is

$$\Delta u(k) = [1 \ 0 \ 0 \ \dots \ 0] \Delta U^*$$

In this case since the Eq. 2 is SISO, the closed loop feedback takes the following form:

$$\begin{aligned} \Delta u(k) &= K_y y_r(k) - K_x x(k) \\ &= -K_x \begin{bmatrix} \Delta x_m \\ y(k) - y_r(k) \end{bmatrix} \end{aligned} \quad (8)$$

The control law to be applied is as below:

$$u(k) = u(k - 1) + \Delta u(k)$$

Finally $i_q^*(k)$ takes the following form

$$i_q^*(k) = \frac{2J}{3P^2 \phi_{mg}} u(k) \quad (9)$$

C) Current controller design

Due to straightforward structure of Eq. 3, it is convenient to apply a simple feedback linearization concept in order to obtaining a zero steady state error for d-q axis current.

The error dynamics of Eq. 3 are shown in the following:

$$\begin{aligned} \dot{e}_{i_q} &= \frac{1}{L_q} (v_q - R e_{i_q} - \omega L_d i_d - \omega \phi_{mg}) - \frac{di_q^*}{dt} \\ &\quad - \frac{R}{L_q} i_q^* \end{aligned} \quad (10)$$

$$\dot{e}_{i_d} = \frac{1}{L_d} (v_d - R e_{i_d} + \omega L_q i_q) - \frac{di_d^*}{dt} - \frac{R}{L_d} i_d^*$$

A suitable choice for the input is performed by utilizing inverse dynamic as the following

$$\begin{aligned} v_q &= \omega L_d i_d + \omega \phi_{mg} + L_q \left(\frac{di_q^*}{dt} + \frac{R}{L_q} i_q^* \right) \\ &\quad - \alpha_q e_{i_q} \end{aligned} \quad (11)$$

$$v_d = -\omega L_q i_q + L_d \left(\frac{di_d^*}{dt} + \frac{R}{L_d} i_d^* \right) - \alpha_d e_{i_d}$$

Where α_q and α_d are the positive constant which larger value result in faster convergence of e_{i_q} and e_{i_d} to the zero.

d) PI controller

As it was mentioned before, PI controllers are widely used for controlling of PMSMs. In this part a PI controllers as the PMSM's position controller is designed. Fig. 4 shows the overall PI strategy. The PI controller gains for both of the position and d and q current controllers has been shown in the table (1).

It must be noted that the PI controller parameters are tuned in a way to achieve the best performance of system outputs.

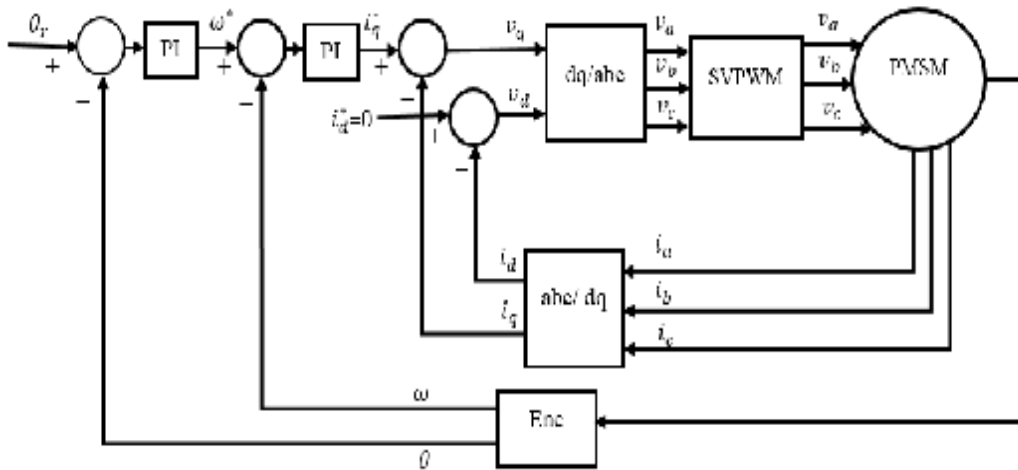


Fig. 4. Overall PI control strategy [5]

Table 1. PI controller parameters

Controller for	K_p	K_i
Position	4	3.16
Speed	316	316

4. Analysis of applied forces to the pedestal

An AZ-EL pedestal uses two motors with the mounted axis correspond to AZ-EL angles. The load torque, itself is composed of two kinds of forces: the gravitational force which depends on the weight of the reflector and pedestal's back structure; and the wind force. These forces vary when the reflector turns around in both azimuth and elevation axis.

In AZ-EL pedestals, one motor rotates the reflector in azimuth direction and the other is in charge of rotating in elevation plate. The elevation angle has a direct impact on the amount of both gravitational and wind forces. When the reflector is placed in a horizontal position, the applied torque is approximately negligible. As the Elevation angle goes towards 0 degrees, the amount of gravitational force increases. The equation (12) models the gravitation force which is applied on the elevation motor in terms of elevation angle:

$$F_{motor-El}^{gravity} = (M_{pedestal} + M_{back\ structure}) \cdot g \cdot \cos(\theta_{El}) \quad (12)$$

It should be noticed that, no force would be applied to the azimuth motor from the gravitational source then

$$F_{motor-Az}^{gravity} = 0 \quad (13)$$

L_1 is considered as length for distance between motor shaft and the center of the reflector, therefore:

$$\tau_{motor1}^{gravity} = (M_{pedestal} + M_{back\ structure}) \cdot g \cdot L_1 \cdot \cos(\theta_{El}) \quad (14)$$

The wind force can be demonstrated in terms of following parameters in Eq. 15

$$F_{wind} = \frac{1}{2} \rho A_f C_D (V + V_{wind})^2 \quad (15)$$

The effective area of the reflector changes as the elevation angle varies. Moreover, the wind force's sign could be changed depending on the azimuth angle of the reflector and wind blowing direction. Therefore, the applied torque on azimuth motor which its source is the wind can be yield through the below relationship:

$$\tau_{motor-Az}^{wind} = \left(\frac{1}{2} \rho A_f C_D (V + V_{wind})^2 \right) \cdot L_1 \cdot \cos(\theta_{El}) \cdot \sin(\theta_{Az} - \delta) \quad (16)$$

Where, δ is the wind blowing direction angle. The applied torque on the elevation motor is obtained in a similar way:

$$\tau_{motor-El}^{max-wind} = \left(\frac{1}{2} \rho A_f C_D (V + V_{wind})^2 \right) \cdot L_1 \cdot \sin(\theta_{El} - \delta) \quad 0 < \theta_{El} < 90 \quad (17)$$

The overall applied torque to each of the motors can be calculated by adding the gravitational and wind torques separately.

5. Pedestal Control System

LEO pedestals are used in order to track a signal source continuously. The desired position of the reflector is sent to the central controller unit. In the next step, desired elevation and azimuth angles are set as the reference position for the two motors of pedestal. Next, the reference will be achieved by applying the proposed control strategy to each PMSM as system's actuators.

6. Simulation Results

Simulation study has been done based on set of sensor data which received from real satellite. The set of real data includes the interval at which the elevation angle passes the zenith angle and the azimuth angle should vary 180 degree suddenly. Table 2 shows the value of parameters of the simulated pedestal system. Control parameters are assigned appropriately and listed in Table 3.

Table 2. Parameters for a Typical Pedestal

Parameter	Value	Parameter	Value
ρ	1.2	Nominal speed	3000 rpm
C_D	0.3	Max. wind speed	90 km/h

Radius of Reflector	150 cm	All mass	501 kg
Nominal torque	2.87n.m	J	2.35×10^{-4}

Table 3. Controller Parameters

Parameter	Value	Parameter	Value
Prediction horizon	5s	R	1
Control horizon	1s	α_q	50
Q	10^5	α_d	50
T_s	10 ms		

To show performance achieved by the proposed control strategy, a comparison between the proposed control strategy and previous PI controller applied to the error dynamics, has been carried out. To this end, Integral Square Error indices in the following form are considered.

$$\begin{aligned}
 ISE_j(k) &= \sum_{i=1}^k E_j^2(k) \tag{16}
 \end{aligned}$$

Reference trajectory tracking of Azimuth and Elevation angles obtained by each controller, is shown in fig. 5 and fig. 6 respectively.

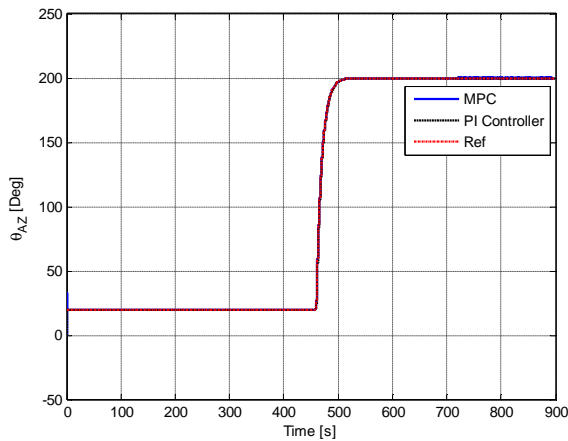


Fig. 5. Azimuth angle reference tracking

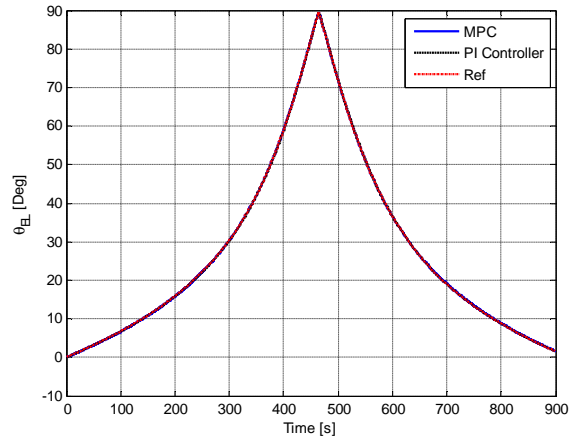


Fig. 6. Elevation angle reference tracking

Corresponding tracking errors is illustrated in fig. 7 and fig. 8, respectively.

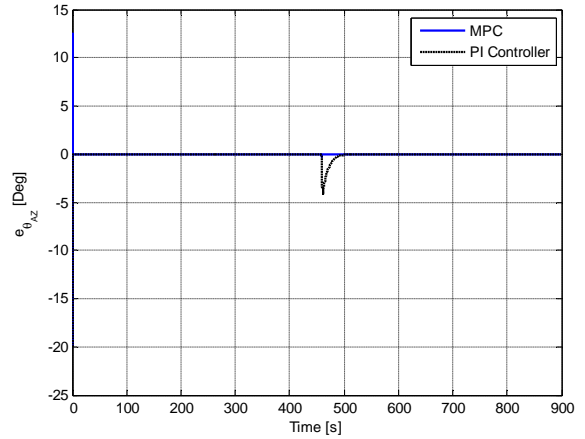


Fig. 7. Azimuth angles tracking error

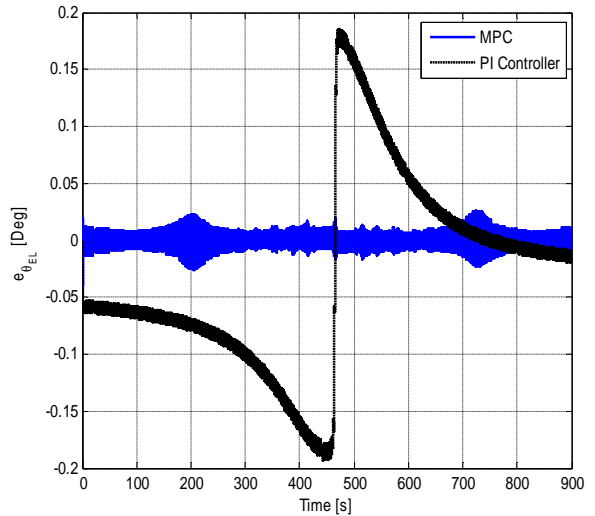


Fig. 8. Elevation angles tracking error

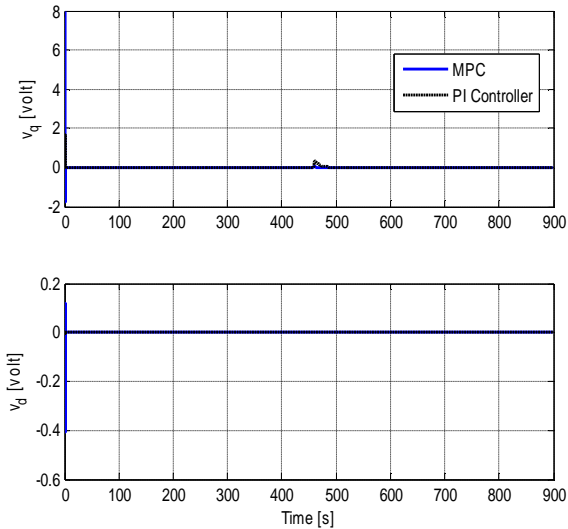


Fig. 9. d-q axis input voltages of Azimuth motor

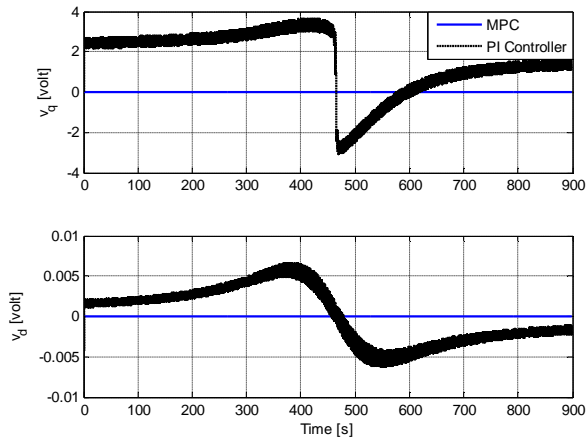


Fig. 10. d-q axis input voltages of Elevation motor

Although, designed control signal through the controllers are depicted in figures 9 and 10.

It is apparent from the designed control signal and trajectory tracking error figures, proposed controller has provided lower energy consumption with better performance, during trajectory tracking mission.

To be more specific, ISE indices is calculated and displayed in figures 11 and 12. As it can be seen, a dramatic improvement achieved by proposed MP controller, especially around the zenith point.

7. Conclusion

In this paper, a nonlinear model of two degree of freedom AZ-EL pedestal without any linearization around the operating points was considered. Two permanent magnet motors were chosen as system actuators. To solve the trajectory tracking problem, a control structure with two general cascade controllers consist of MPC for position and nonlinear FL to regulate the current was developed

for each of PMSMs. The applied forces on each pedestal’s actuator, gravitational and

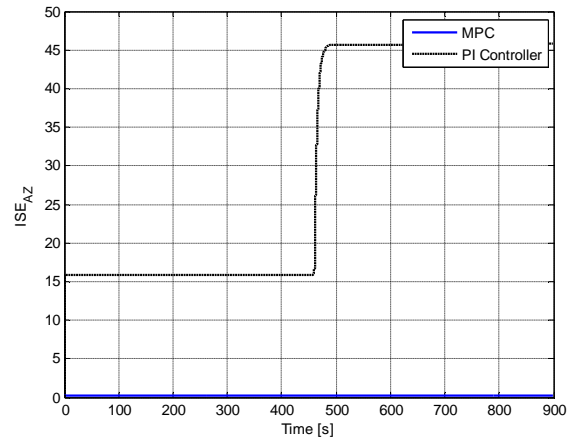


Fig. 11. ISE indices for $e_{\theta_{AZ}}$

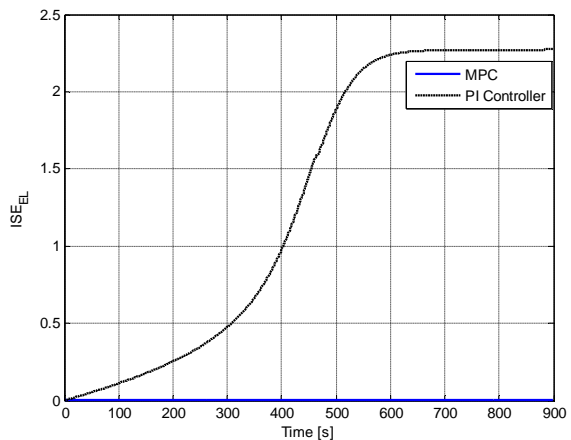


Fig. 12. ISE indices for $e_{\theta_{EL}}$

wind forces were analysed and modelled for an AZ-EL pedestal. Parameters of a real pedestal and atmospheric conditions, such as wind speed, were considered during simulation.

Finally, to show the improvements achieved by the proposed control strategy, a comparison between the proposed control

strategy and previous PI controller, was carried out. In this way, a numerical analysis was performed by employing ISE indices. The better performance and robustness of proposed method with respect to the unknown disturbance was demonstrated. Results approved the effectiveness of the proposed controller.

8. Reference

[1] K. Willey, Selecting a Pedestal for Tracking LEO Satellites at Ka Band. Microwave journal, Vol. 12, pp. 234-239, 2000.
 [2] C. H. Looney, and D. J. G. Carlson, Coverage diagrams for X-Y and elevation-aver-azimuth

- antenna mounts, Space Flight Center, Greenbelt, MD, USA, Tech. Rep. D-2963, Aug. 1965
- [3] A. J. Rolinski, D. J. Carlson, and R. J. Coates, Satellite-tracking characteristics of the X-Y mount for data acquisition antennas, Goddard Space Flight Center, Greenbelt, MD, USA, Tech. Rep.D-1697, Jun. 1964.
- [4] H. B. Shin. New anti windup PI controller for variable-speed motor drives. *IEEE Transactions on Industrial Electronics*, 45(3), 445–450, 1998.
- [5] A. R. Ghafari Kashani, J. Faiz, M.J. Yazdanpanah, Integration of nonlinear HI and sliding mode control techniques for motion control of a permanent magnet synchronous motor, *IET Electric Power Applications*. 2009.
- [6] K. H. Kim and M. J. Youn, A nonlinear speed control for a PMSM using a simple disturbance estimation technique, *IEEE Trans., Ind., Electron.*, vol. 49, no. 3, pp. 524–535, Jun. 2002.
- [7] B. Grçar, P. Cafuta, M. Znidaric, and F. Gausch, Nonlinear control of synchronous servo drive, *IEEE Trans., Control Syst. Technol.*, vol.4, no. 2, pp. 177–184, Mar. 1996.
- [9] H. Z. Jin and J. M. Lee, An RMRAC current regulator for permanent magnet synchronous motor based on statistical model interpretation, *IEEE Trans., Ind., Electron.*, vol. 56, no. 1, pp. 169–177, Jan. 2009.
- [10] Y. A.R. I. Mohamed, Design and implementation of a robust current-control scheme for a PMSM vector drive with a simple adaptive disturbance observer, *IEEE Trans., Ind., Electron.*, vol. 54, no. 4, pp. 1981–1988, Aug. 2007.
- [11] Y. A. R. I. Mohamed and E. F. Saadany, A current control scheme with an adaptive internal model for torque ripple minimization and robust current regulation in PMSM drive systems, *IEEE Trans., Energy Convers.*, vol. 23, no. 1, pp. 92–100, Mar. 2008.
- [12] T. L. Hsien, Y.-Y. Sun, and M.-C. Tsai, H-infinity control for a sensor less permanent magnet synchronous drive, *Proc. Inst., Elect. Eng., Electr. Power Appl.*, vol. 144, no. 3, pp. 173–181, May 1997.
- [13] I. C. Baik, K. H. Kim, and M. J. Youn, Robust nonlinear speed control of PM synchronous motor using boundary layer integral sliding mode control technique, *IEEE Trans., Control Syst., Technol.*, vol. 8, no. 1, pp. 47–54, Jan. 2000.
- [14] R. J. Wai, Total sliding-mode controller for PM synchronous servo motor drive using recurrent fuzzy neural network, *IEEE Trans., Ind., Electron.*, vol. 48, no. 5, pp. 926–944, Oct. 2001.
- [15] B. Grçar, P. Cafuta, M. Znidaric, and F. Gausch, Nonlinear control of synchronous servo drive, *IEEE Trans., Control Syst., Technol.*, vol.4, no. 2, pp. 177–184, Mar. 1996.
- [16] D. M. Vilathgamuwa, M. A. Rahman, K. Tseng, and M. N. Uddin, Nonlinear control of interior permanent magnet synchronous motor, *IEEE Trans., Ind., Appl.*, vol. 39, no. 2, pp. 408–416, Mar. Apr. 2003.
- [17] J. Zhou and Y. Wang, Adaptive backstepping speed controller design for a permanent magnet synchronous motor, *Proc. Inst. Elect. Eng., Electr. Power Appl.*, vol. 149, no. 2, pp. 165–172, Mar. 2002.
- [18] Y.-S. Kung and M.-H. Tsai, FPGA-based speed control IC for PMSM drive with adaptive fuzzy control, *IEEE Trans. Power Electron.*, vol. 22, no. 6, pp. 2476–2486, Nov. 2007.
- [19] Wang, L., & Gan, L. Gain scheduled continuous-time model predictive controller with experimental validation on ac machine. *International Journal of Control*. 2013.
- [20] L. Wang, *Model predictive control system design and implementation using MATLAB* (1st ed). London: Springer. 2009.
- [21] E. Camacho & C. Bordons, *Model predictive control*. New York: Springer-Verlag, 2007, ch. 2.
- [22] Y. Wang, J. Fei, adaptive fuzzy sliding mode control for PMSM position regulation system, *International Journal of Innovative computing, Information and Control*, Vol 11, June 2015.